CONF-920146--6

DE93 001374

FRACTURE TOUGHNESS MEASUREMENTS WITH SUBSIZE DISK COMPACT SPECIMENS*

David J. Alexander

Metals and Ceramics Division
OAK RIDGE NATIONAL LABORATORY
Oak Ridge, TN 37831-6151

ASTM SYMPOSIUM ON SMALL SPECIMEN TEST TECHNIQUES AND THEIR APPLICATION TO NUCLEAR REACTOR VESSEL THERMAL ANNEALING AND PLANT LIFE EXTENSION

January 29-31, 1992
New Orleans, Louisiana

---

*Research sponsored by the Office of Fusion Energy, U.S. Department of Energy, under contract DE-AC05-84OR21400 with Martin Marietta Energy Systems, Inc.

TITLE OF SYMPOSIUM:

ASTM Symposium on Small Specimen Test Techniques and Their Application to Nuclear Reactor Vessel Thermal Annealing and Plant Life Extension, January 29-31, 1992, New Orleans, Louisiana

AUTHOR:

David J. Alexander[1]

TITLE OF PAPER:

Fracture Toughness Measurements with Subsize Disk Compact Specimens

AUTHOR'S AFFILIATION:

[1]Development Staff Member, Metals and Ceramics Division, Oak Ridge National Laboratory, 4500S, MS-6151, P.O. Box 2008, Oak Ridge, TN 37831-6151

ABSTRACT: Special fixtures and test methods have been developed for testing small disk compact specimens (12.5 mm diam by 4.6 mm thick). Both unloading compliance and potential drop methods have been used to monitor crack extension during the J-integral resistance (J-R) curve testing. Provisions have been made to allow the necessary probes and instrumentation to be installed remotely using manipulators for testing of irradiated specimens in a hot cell. Laboratory trials showed that both unloading compliance and potential drop gave useful results. Both techniques gave similar data, and predicted the final crack extension within allowable limits. The results from the small disk compact specimens were similar to results from conventional compact specimens 12.7-mm thick. However, the slopes of the J-R curves from the larger specimens were lower, suggesting that the smaller disk compact specimens may have lost some constraint due to their size. The testing shows that it should be possible to generate useful J-R curve fracture toughness data from the small disk compact specimens.

KEY WORDS: disk compact specimen, fracture toughness, irradiation effects, test methods, unloading compliance, potential drop, crack extension, J-integral resistance curves, J-R curves, clip gage

Introduction

Candidate materials are being evaluated for the first-wall structure in the International Thermonuclear Experimental Reactor (ITER). Current estimates of the operating temperatures indicate that the structure will operate below about 300°C. One of the materials proposed for the first wall is type 316 stainless steel. Very little information is available on the effects of irradiation at these low temperatures on the mechanical properties of austenitic stainless steels, particularly the fracture toughness [1]. Therefore, work is under way at Oak Ridge National Laboratory (ORNL) to measure the effect of irradiation on the fracture toughness of a variety of austenitic stainless steels. This paper describes some of the techniques that have been developed for this testing, and presents some preliminary results from unirradiated material and comparisons with larger conventional specimens.

The irradiations for these experiments are being conducted at the High-Flux Isotope Reactor (HFIR) at ORNL due to the reactor availability and the high fluxes present in the HFIR target region. However, achieving the necessary low irradiation temperatures (60 and 300°C) placed severe restrictions on the specimen geometry. The gamma heating from the high-flux irradiation and the limited cooling available from the reactor cooling water required a very small specimen size to attain the lowest irradiation temperature. To use the HFIR target region efficiently, it was necessary to adopt a circular specimen geometry for the fracture toughness specimens. Therefore, the disk compact specimen geometry was chosen. This is an accepted specimen geometry for K_{Ic} measurements (ASTM Standard Test Method for Plane-Strain Fracture Toughness of Metallic Materials, E 399-90), but is not yet included in the standards for J-integral-resistance (J-R) curve testing (ASTM Standard Test Method for J_{Ic}, A Measure of Fracture Toughness, E 813-89, or ASTM Standard Test Method for Determining J-R Curves, E 1152-87). These standards presently allow only conventional rectangular compact specimens or bend bars; however, the disk and rectangular compact specimens are very similar in geometry, and J-R data can be correctly determined from each if the appropriate compliance expressions are used. Preliminary experiments [2] indicated that useful data could be generated in the laboratory from small disk compact specimens.

The heat transfer calculations performed at ORNL and the size limitations imposed by the HFIR target region characteristics resulted in the selection of a specimen diameter and thickness of 12.5 and 4.63 mm (0.492 and 0.182 in.), respectively. This very small specimen size would demand special techniques for testing.

There are two conventional methods employed in J-R testing for monitoring crack growth during the test: unloading compliance, and potential drop. Unloading compliance (UC) requires periodic partial unloadings of the specimen to determine the specimen compliance, from which the crack length and extension are calculated. This technique demands high accuracy for the measurement of the load-displacement data in order to determine the correct compliance values, and hence crack extensions. The second method, potential drop (PD), imposes a constant current across the specimen and measures the changing resistance of the unbroken ligament as the crack extends. This resistance change is used to determine the crack length. Less accurate displacement measurements are necessary than with UC testing, as the displacement is used only to calculate the energy required for crack extension, and this calculation is less sensitive to the displacement measurement than are the compliance measurements necessary for UC determination of crack growth. UC measurements for irradiated specimens have been successfully done at ORNL, and much more experience had been accumulated in testing unirradiated material with UC than with PD. However, the small specimen size precluded the use of conventional displacement measuring methods available at ORNL, so it was decided to pursue both the UC and the PD techniques, in case one of the methods proved to be impractical for remote testing in a hot cell.

Test Methods

The UC technique requires accurate measurement of the specimen displacements. The usual technique for measuring the displacements along the specimen load line is to fabricate the specimen with a cutout that allows a clip gage to be inserted between the loading pin holes to the load line, where it seats on knife edges fastened along the load line on the sides of the notch cutout. An example of the resultant specimen geometry is shown in Fig. 1 for a compact specimen 12.7-mm-thick

(0.5-in.) [designated 0.5 T C(T)]. However, the disk compact specimen is much smaller, with a thickness of only 4.6 mm (0.18 in.). [This disk compact specimen is thus designated 0.18 T DC(T)]. As a result, there is not sufficient room between the loading holes for a cutout to allow a clip gage to be inserted to the load line. Therefore, grooves were machined on the outer edge of the specimen above and below the loading holes (see Fig. 1) so that the load line displacement could still be measured directly, but outside the loading holes rather than in between them. The grooves had an included angle of 60°, with a depth of 0.5 mm (0.020 in.) and a root radius of 0.05 mm (0.002 in.). A robust and rugged yet highly accurate clip gage that could be handled by manipulators was designed. The gage included knife edges that would seat in the grooves. This clip gage, termed an "outboard" gage since it was attached outside of the loading holes, contained a central flexural beam on which four strain gages were attached for a full-bridge measurement of the strains and hence the displacement. Figure 2 shows the outboard gage attached to one of the disk compact specimens.

There appeared to be only two drawbacks to the outboard gage: possible difficulties in using manipulators to remotely mount the gage on the specimens, and possible damage to the gage if the specimen fractured suddenly during testing. Trials in the hot cells have shown that the gage can be handled with manipulators, and the knife edges seated in the specimen grooves. The problem of gage damage was addressed by providing overtravel stops on the back end of the gage. Hopefully, if the specimen did suddenly fracture and the servohydraulic test machine did not prevent a rapid separation of the grips and opening of the gage, the stops would prevent the central flexural beam from being permanently deformed and damaged. It was hoped that the knife edges would either slip out of the grooves, or perhaps break off where they are attached to the gage arms, thus preventing damage to the gage.

The PD setup presented much greater difficulties. Four probes would have to be attached to each specimen: two for the constant current, and two to monitor the changing voltage drop across the specimen ligament. Current input and output locations were chosen at the top and bottom of the specimen along the centerline, and the crack monitoring probes were located 15° above and below the crack plane, on the front edge of the specimen, where drilled and tapped holes could be located

without damaging the loading holes. It was decided to forgo two additional probes for a reference measurement to reduce the number of connections that would have to be made in the hot cell. Instead, a second specimen would be connected in series with the test specimen, and the crack monitor signal from the dummy specimen would be used for a reference signal.

A PD calibration function was developed from measurements on thin aluminum mockups of the disk compact geometry. The specimen diameter was increased to 137.2 mm (5.4 in.) but the thickness was 3.2 mm (0.125 in.). Crack extension was simulated by slitting with a thin saw blade. The current and voltage readings were recorded at increments in the crack length to specimen width ratio (a/W) of about 0.05, for a/W values from 0.25 (the initial machined notch depth) to roughly 0.9. The voltage values were then normalized by the voltage value at a/W of 0.25, and fit with a third-order polynomial, given by

$$a/W = -0.261198+0.6237(V/V_o)-0.118315(V/V_o)^2+0.008512(V/V_o)^3 , \quad (1)$$

where a/W is the crack length, V is the measured voltage, and V_o is the voltage for the specimen at a crack length of a/W = 0.25. This gave a correlation coefficient greater than 0.9999. During testing, an uncracked specimen would be used for the reference measurement to provide the value of the voltage at a/W = 0.25.

Attaching the probes would be simple in the laboratory, but much more difficult remotely in the hot cell. A fixture and special tools were designed to assist the manipulator operators in this task (Fig. 3). The specimen would be located in a special fixture to align the predrilled and tapped holes in the specimen with the threaded probes. The fixture would prevent the probes from being cross-threaded. The initial prototype of the fixture was machined from clear plexiglass simply for expediency; however, it was realized that the transparency of the plastic was helpful in the assembly and desirable. The stainless steel probes were machined with hex heads, and a nutdriver would be used to attach them. The sequence of operations required to attach the probes is shown in Fig. 4. The top half of the fixture has been removed for clarity. The specimen would be placed in the central

recess [Fig. 4(a)], and a thin piece of shim stock (omitted for clarity) would be inserted in the fixture slit and the specimen notch to properly align the specimen. The original proposal suggested that the probes be placed into the appropriate hole as shown in Fig. 4(b), but it was realized that a better method would be to first load the probe into the shaft of the nutdriver, which was drilled out to allow the probe to slide into the nutdriver until the hex flats were engaged. The nutdriver would be inserted into the appropriate hole [Fig. 4(c)] and then rotated until the probe was secured. The process would be repeated until all four probes were attached [Fig. 4(d)]. The specimen and probes would then be removed from the fixture [Fig. 4(e)]. The final step would be to attach the proper leads to the probes [Fig. 4(f)]. The leads would have fittings designed to slide onto the probes. The fittings on the leads were obtained by stripping the plastic coating from female banana plugs and soldering the internal connector to the lead wires. The probe diameters matched the corresponding male banana plugs. This provided an effective electrical connection that could be assembled with manipulators.

The nutdriver for attaching the probes is shown in Fig. 5. To facilitate handling the nutdriver, cross pieces were added to the handle by drilling through two offset holes 90° apart near the end of the handle, and pressing thin rods through these holes. These cross pieces prevent the nutdriver from rolling when it is laid down, and also hold the handle of the nutdriver up so that the manipulator can easily grasp the nutdriver. The primary function of the cross pieces is to allow the nutdriver to be rotated for screwing in the probes. An additional modification was the addition of a slip coupling with an adjustable torque setting to the shaft of the nutdriver (Fig. 5). The slip coupling was inserted by cutting the shaft of the nutdriver near the handle. A suitable torque level was determined by trial and error in the laboratory. The slip coupling would prevent inadvertent overtightening and twisting off of the fragile threaded probes as they were attached to the specimen. This would be very likely with the manipulators necessary for the attachment, as they do not transmit much "feel" back to the manipulator operator.

The completed assembly of the probes and clip gage on the specimen is shown in Fig. 6. This entire assembly would then be inserted into clevises for the fracture testing. The clevises would have a wider and deeper slot than normal, to facilitate the insertion of the specimen assembly with

manipulators. This would also reduce the likelihood of accidental contact of the leads with the legs of the clevises that would result in changes in the electrical signals, or rubbing of the clip gage against the clevis that would distort the displacement measurements.

The disk compact specimen and the outboard clip gage have been successfully mounted in the load train of the servohydraulic test machine in the hot cell, using manipulators. No additional fixturing was required to align the specimen assembly with the grips so that the loading pins could be inserted. The pins were made with one end tapered and an offset block on the other end for handling with the manipulator. The clip gage was first attached to the specimen, and examined to be sure that the knife edges were seated in the grooves. The operator then grasped one arm of the clip gage with the manipulator and inserted the specimen in the load train. Inserting the pins through the loading holes was difficult, but was possible without needing special fixtures. No attempt has been made to attach the PD leads in the hot cell.

Laboratory Trials and Discussion of Results

Several trials have been conducted in the laboratory to compare the UC and PD techniques on the 0.18 T DC(T) specimens, and to compare these results to UC data from 0.5 T C(T) specimens of the same material. Specimens of both geometries were machined from the same 14-mm-thick (0.55-in.) plate of annealed type 316 stainless steel from the National Fusion Reference Heat X15893. The specimens were oriented in the T-L orientation so that crack growth was in the rolling direction. All specimens were taken from the center of the plate thickness. The specimens were precracked at room temperature with a final maximum stress intensity of approximately 22 MPa$\sqrt{m}$ (20 ksi$\sqrt{in.}$). A chevron notch was used for both specimens to assist crack initiation and maintain crack front straightness during precracking. The DC(T) and C(T) specimens were precracked to nominal a/W values of 0.5 and 0.6, respectively. The specimens were then side grooved 10% of their thickness on each side (20% total) with an included angle of 45° and a root radius of 0.25 mm (0.010 in.) or 0.10 mm (0.004 in.) for the C(T) and DC(T) specimens, respectively. The sidegrooves would suppress the development of slant shear fracture.

All tests were conducted at room temperature, and the manufacturer's values of 260 and 560 MPa (38 and 81 ksi) were used for the yield and ultimate tensile strengths, respectively, in calculating the blunting lines for the data analyses. Values of 193 GPa (28 000 ksi) and 0.3 were assumed for the elastic modulus and Poisson's ratio, respectively. Tests were conducted in general accordance with E 813-89 and E 1152-87 using a computer-controlled testing and data acquisition system described elsewhere [3]. After completion of the test, the specimens were heat tinted to mark the final crack position by placing them on a hot plate and heating them until a noticeable color change was evident. The specimens were then cooled to room temperature and broken open. The initial and final crack lengths were measured with the aid of a measuring microscope, and the crack lengths were calculated by the nine-point average method.

An electrical isolation grip was used in the top of the loading train to insure that the test machine would not provide an alternate current path for the potential during the testing. Measurements of the potential showed that attaching the clip gage resulted in a slight shift (about 2%) in the apparent crack length calculated from the potential drop, due to current travelling through the body of the clip gage. No correction was made for this small error.

A problem with the analysis of potential drop measurements is the determination of the initiation of crack growth. There may be significant changes in the potential drop signal prior to actual crack growth. In order to determine when crack growth begins, during the analysis routine the voltage ratio (the potential of the test specimen divided by the potential from the reference specimen) is plotted against the load line displacement. A typical example is shown in Fig. 7. There is an initial linear portion, with a subsequent deviation from this linearity. This deviation from linearity is taken as the beginning of crack extension [4-6]. During the posttest analysis, the computer program allows the operator to interactively position a straight line through the data to assist in determining the initial deviation from linearity. The data prior to this point are assigned to the calculated blunting line, and crack extension is then calculated from this point on. As Fig. 7 shows, this material showed a sharp and distinct break, making the choice for the beginning of crack extension a simple one. The potential drop data shown in Fig. 7 are the average of sixty readings of the voltage taken during

pauses in the test while the computer program performed calculations for the unloading compliance testing. Data were also taken continuously during the test, and showed excellent agreement with the data taken during the pauses.

The UC and PD data gave very similar results for the DC(T) specimens. An example of the results is shown in Fig. 8. Both techniques show similar final crack extensions, and predicted the measured final crack extension to within the 15% allowed by ASTM E 813-89. This excellent agreement between the two techniques provided further justification for the method used to determine the initiation of crack growth from the potential drop data. The load-displacement curves showed little or no hysteresis during the unload-load cycles until near the end of the test. The cause of this hysteresis late in the test is unclear. It may be caused by the knife edges contacting the sides of the grooves as the specimen opens, or by rotation of the loading pins causing them to ride up the sides of the pin holes in the grips, although loading flats were provided in the clevises. Neither of these possibilities seems very likely, as the specimens fractured without gross changes of geometry. Perhaps 90° grooves would be better than the 60° used for these specimens. This problem will be examined with additional testing, although it does not seem to have harmed the quality of the data.

The material tested showed some scatter in the toughness, as is shown in Fig. 9. These identical specimens show very different fracture behaviors. Specimen DC9 shows a greater J_{Ic} value and a higher J-R curve than does specimen DC2. The fracture toughness and tearing modulus values from all of the specimens tested are shown in Table 1. This table also includes the results from the 0.5 T C(T) specimens.

The thicker C(T) specimens gave results similar to the low toughness DC(T) specimens. In general, the J_{Ic} values were similar, but the J-R curves for the thicker specimens were flatter, giving lower values of the tearing modulus (see Table 1). A comparison of the results for the two specimens types is shown in Fig. 10.

The toughness values are surprisingly low for an annealed austenitic stainless steel. The tearing modulus values measured with the C(T) specimens are also very low. This low resistance to fracture resulted in very little distortion of the specimens. The fracture surfaces from two of the disk

compact specimens are shown in Fig. 11. The low toughness resulted in very flat fracture surfaces and very little lateral contraction of the specimens ahead of the crack front. This lack of change in the specimen geometry may have helped the agreement between the different specimen types. The low toughness favors fracture rather than the growth of a large plastic zone. A large plastic zone would have relieved the stresses ahead of the crack tip, and interacted more readily with the edges of the small disk compact than with those of the larger compact specimen, for similar levels of stress intensity. Thus, the good agreement between these two specimen types may not extend to tougher materials. Further trials are planned with a tougher material. However, the good agreement between the two specimen types is very encouraging for the planned irradiation program, as the irradiation is expected to result in high strength and low toughness for the stainless steels. Thus the small disk compact specimen should provide useful data.

Conclusions

Special tools, fixtures, and instrumentation have been developed to permit both UC and PD measurements to be made on small disk compact specimens. The techniques are apparently suitable for remote operation with manipulators. Laboratory trials have shown that both methods give similar results. In addition, these results are in good agreement with results from UC testing of larger conventional compact specimens. These methods will be used to determine the effects of low-temperature irradiation on the fracture toughness of candidate stainless steel alloys for the first wall of a fusion reactor.

Acknowledgments

Research sponsored by the Office of Fusion Energy, U.S. Department of Energy, under contract DE-AC05-84OR21400 with Martin Marietta Energy Systems, Inc. The clip gage was designed and fabricated by John A. Shepic, Lakewood, CO 80228. The slip coupling was purchased from Winfred M. Berg, Inc., East Rockaway, NY 11518. We would like to thank L. J. Turner and A. E. Parker for helpful suggestions for modifications to assist handling with the manipulators. The fracture toughness testing was performed by R. L. Swain, and M. J. Swindeman and J. J. Henry, Jr., performed the potential drop calibration experiments with a system assembled by D. L. Thomas from the Instrumentation and Controls Division, ORNL. The manuscript was reviewed by R. W. Swindeman, D. E. McCabe, and R. K. Nanstad, and prepared by J. L. Bishop.

References

[1] G. R. Odette and G. E. Lucas, "Effects of Low Temperature Neutron Irradiation on the Properties of 300 Series Stainless Steels," *Fusion Reactor Materials Semiannual Progress Report for Period Ending March 31, 1989*, DOE/ER-0313/6, DOE Office of Fusion Energy, p. 313.

[2] C. Elliot, M. Enmark, G. E. Lucas, G. R. Odette, and A. F. Rowcliffe, "Development of Disc Compact Tension Specimens and Test Techniques for HFIR Irradiations," *Fusion Reactor Materials Semiannual Progress Report for Period Ending September 30, 1990*, DOE/ER-0313/9, DOE Office of Fusion Energy, p. 7.

[3] R. K. Nanstad, D. J. Alexander, R. L. Swain, J. T. Hutton, and D. L. Thomas, "A Computer-Controlled Automated Test System for Fatigue and Fracture Testing," *Applications of Automation Technology to Fatigue and Fracture Testing, ASTM STP 1092*, A. A. Braun, N. E. Ashbaugh, and F. M. Smith, Eds., American Society for Testing and Materials, Philadelphia, 1990, p. 7.

[4] J. M. Lowes and G. D. Fearnehough, "The Detection of Slow Crack Growth in Crack Opening Displacement Specimens Using an Electrical Potential Method," *Engineering Fracture Mechanics*, Vol. 3, 1971, p. 103-108.

[5] M. G. Vassilaros and E. M. Hackett, "J-Integral R-Curve Testing of High Strength Steels Utilizing the Direct-Current Potential Drop Method," *Fracture Mechanics: 15th Symposium, ASTM STP 833*, R. J. Sanford, ed., American Society for Testing and Materials, Philadelphia, 1984, p. 535.

[6] E. M. Hackett, M. T. Kirk, and R. A. Hays, *An Evaluation of J-R Curve Testing of Nuclear Piping Materials Using the Direct-Current Potential Drop Technique*, NUREG/CR-4540, U.S. Nuclear Regulatory Commission, Washington, D.C., August 1984.

Table 1--Fracture toughness results

Specimen number	Specimen type	Crack extension method[a]	J_Q		K_J		Tearing modulus	Crack extension agreement[b] (%)
			(kJ/m^2)	(in.-lb/in.^{2})	(MPa$\sqrt{m}$)	(ksi$\sqrt{in.}$)		
DC5[c]	Disk compact	UC	63	356	110	100	15	-9.0
DC9	Disk compact	UC	58	329	106	96	22	-9.6
DC2	Disk compact	UC	36	207	84	76	24	-10.0
	Disk compact	PD	38	218	86	78	23	-14.8
DC16	Disk comapct	UC	46	262	94	86	17	-13.4
	Disk compact	PD	44	254	93	84	21	-17.0
CT04	Compact	UC	36	203	83	75	10	-13.8
CT07	Compact	UC	34	196	81	74	18	-10.0

[a]UC = unloading compliance; PD = potential drop.
[b]Negative agreement indicates predicted crack extension was less than actual measured crack extension.
[c]Noticeable backup (apparent negative crack extension) reported at beginning of test.

Figure Captions

FIG. 1--A comparison of a conventional 1/2 T compact specimen (left) and the 0.18 T disk compact specimen (right). Note the cutout in the compact specimen to allow a clip gage to be inserted to the load line between the loading holes. The disk compact has notches outside the loading holes for the outboard clip gage.

FIG. 2--The outboard clip gage seated on the disk compact specimen. The central flexural beam has four strain gages for the measurement of the displacements. The back end of the gage will allow handling with a manipulator. The gap at the rear of the gage is designed to provide overtravel protection if the specimen fractures suddenly during testing.

FIG. 3--The fixtures, probes, and tools used for assembly of the potential drop setup.

FIG. 4--The sequence of operations required for the attachment of the potential drop probes to the disk compact specimen.

FIG. 5--The modified nutdriver used for attaching the probes to the disk compact specimen. Note the cross pieces at the end of the handle, and the slip coupling inserted on the shaft.

FIG. 6--A view of the complete assembly, showing the potential drop probes and lead wires, and the unloading compliance clip gage. The clip gage has a protective shield mounted over the middle flexural member, to protect the strain gages.

FIG 7--A plot of the voltage ratio versus the load line displacement for one of the disk compact specimens. The straight line is used to assist the selection of the point of initial deviation from linearity. The vertical line shows the point selected as the beginning of crack extension.

FIG. 8--An example of the J-R curves from a disk compact specimen, showing excellent agreement between the data from unloading compliance and that from potential drop. Both methods predict the measured final crack extension (shown by the vertical dashed line) quite well. The solid triangles show the calculated critical J values.

FIG. 9--J-R curves obtained by the unloading compliance technique from two apparently identical disk compact specimens, showing that some scatter was observed from replicate tests. Both tests showed good agreement between measured and predicted crack extensions.

FIG. 10--A comparison between the J-R curves obtained by unloading compliance from 1/2 T compact specimens and the 0.18 T disk compact specimens. The compact specimens gave similar J_{ic} values, but the J-R curves had lower slopes (lower tearing moduli).

FIG. 11--Fracture surfaces from two of the disk compact specimens. Note the chevron notch to assist in precracking, and the sidegrooves added after precracking was finished. The fracture surface shows that crack growth occurred with slight tunneling, but there was little distortion of the specimens' shape.

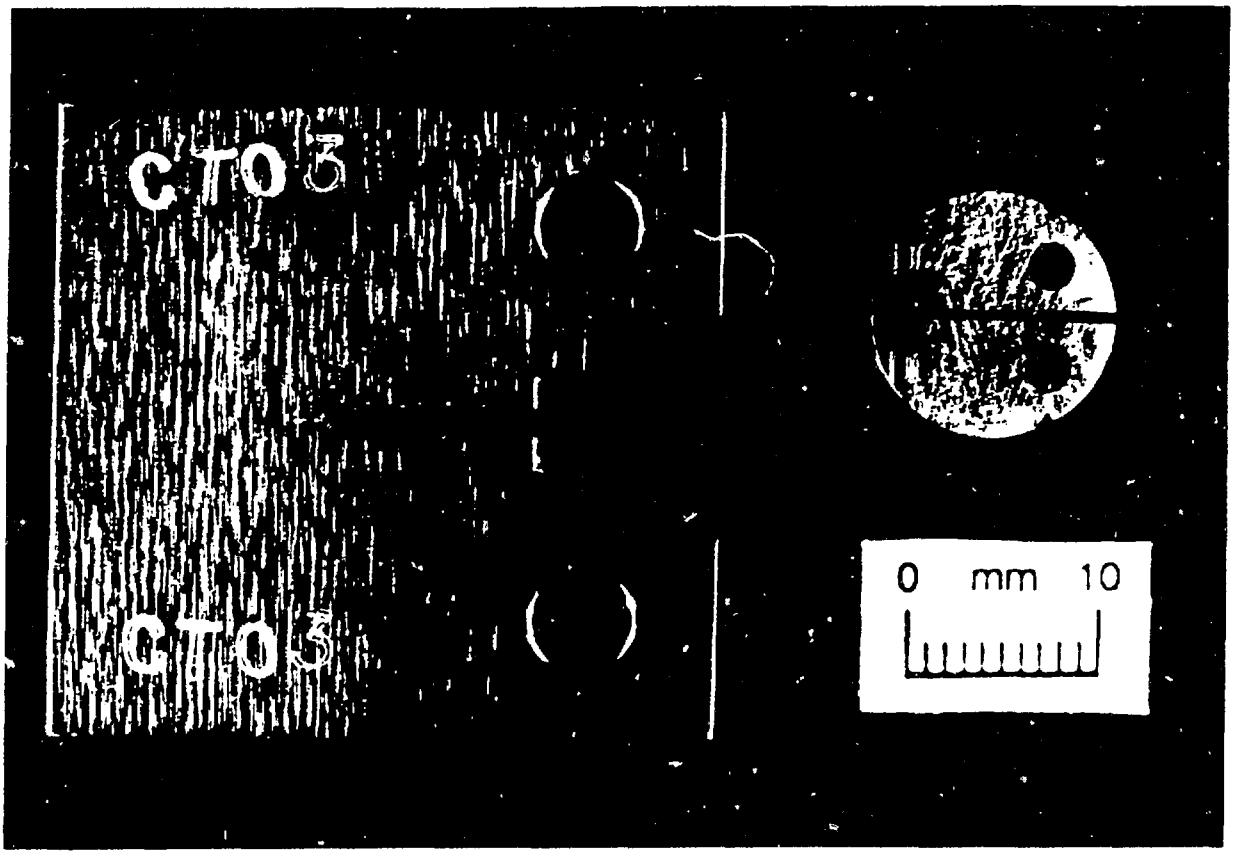

Fig. 1. A comparison of a conventional 1/2 T compact specimen (left) and the 0.18 T disk compact specimen (right). Note the cutout in the compact specimen to allow a clip gage to be inserted to the load line between the loading holes. The disk compact has notches outside the loading holes for the outboard clip gage.

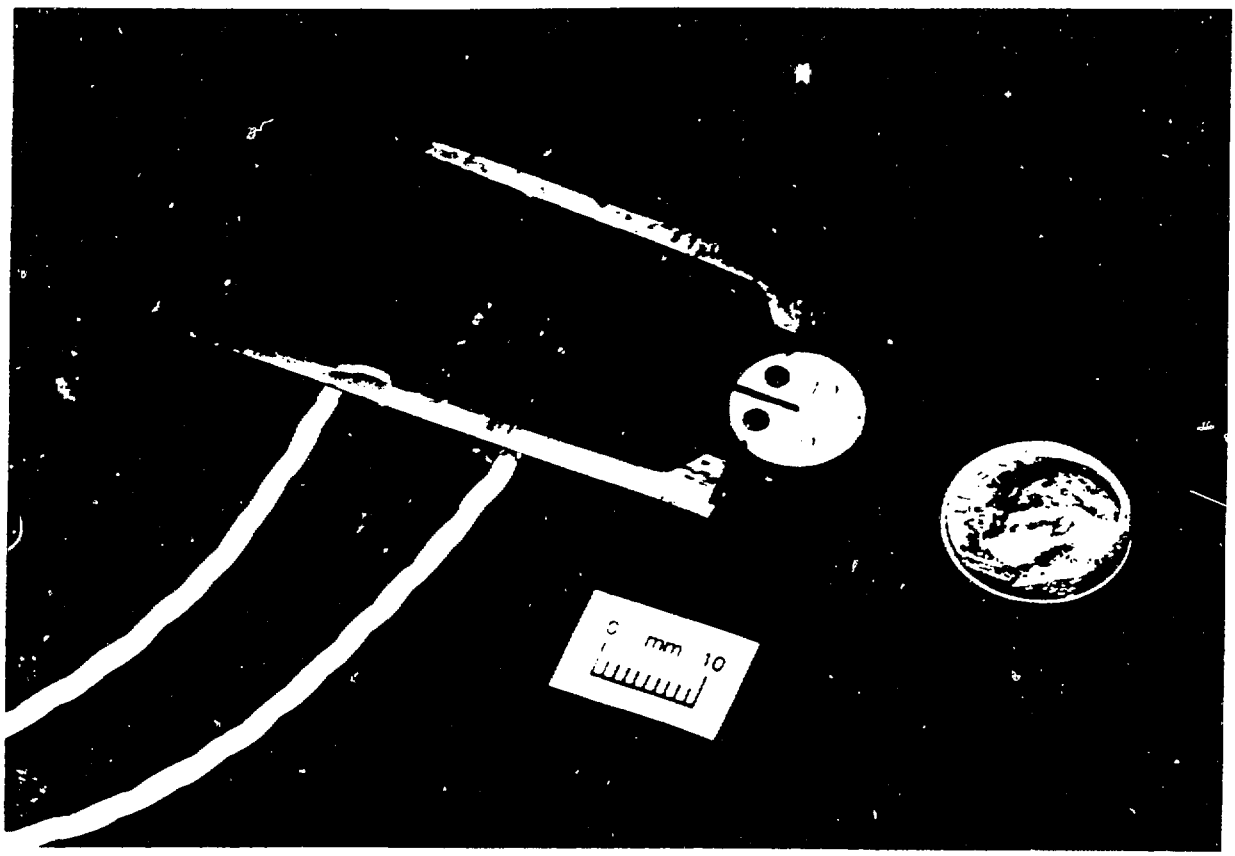

Fig. 2. The outboard clip gage seated on the disk compact specimen. The central flexural beam has four strain gages for the measurement of the displacements. The back end of the gage will allow handling with a manipulator. The gap at the rear of the gage is designed to provide overtravel protection if the specimen fractures suddenly during testing.

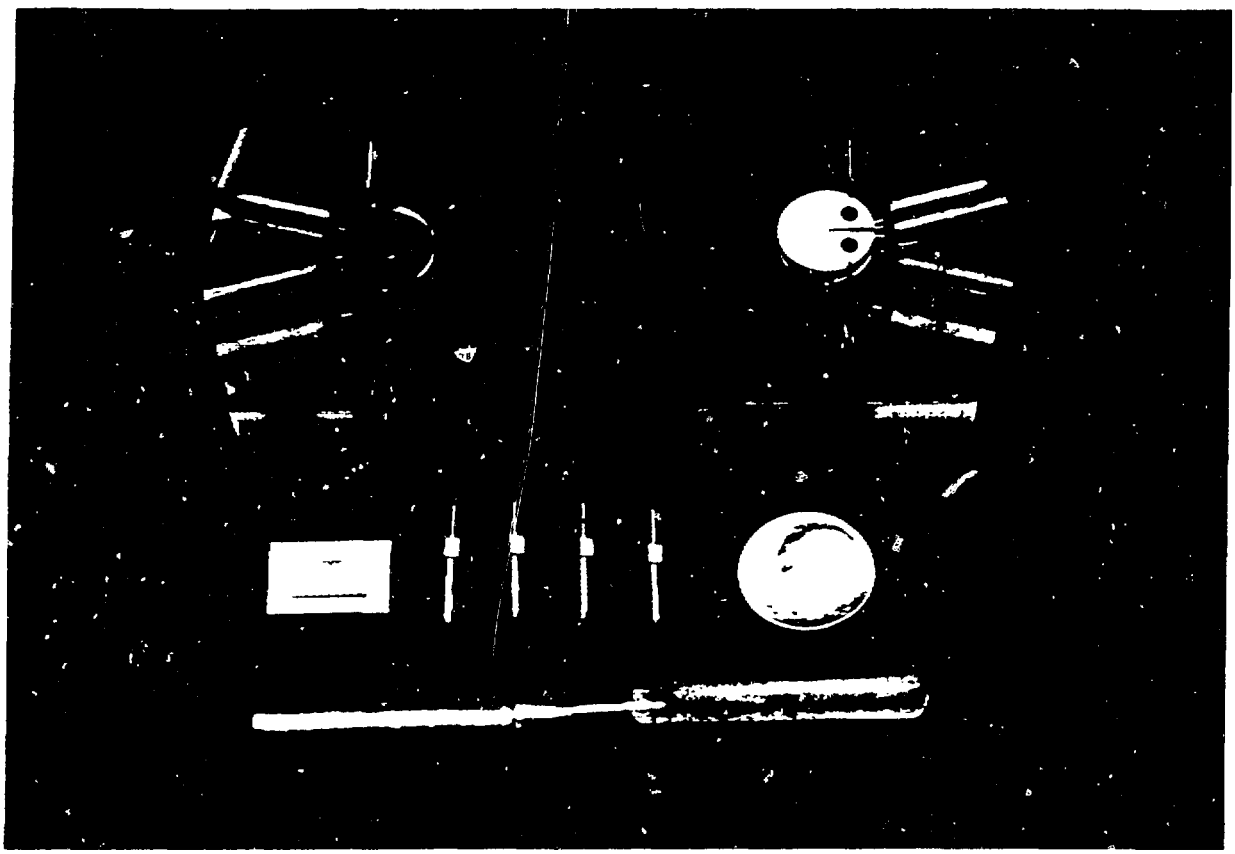

Fig. 3. The fixtures, probes, and tools used for assembly of the potential drop setup.

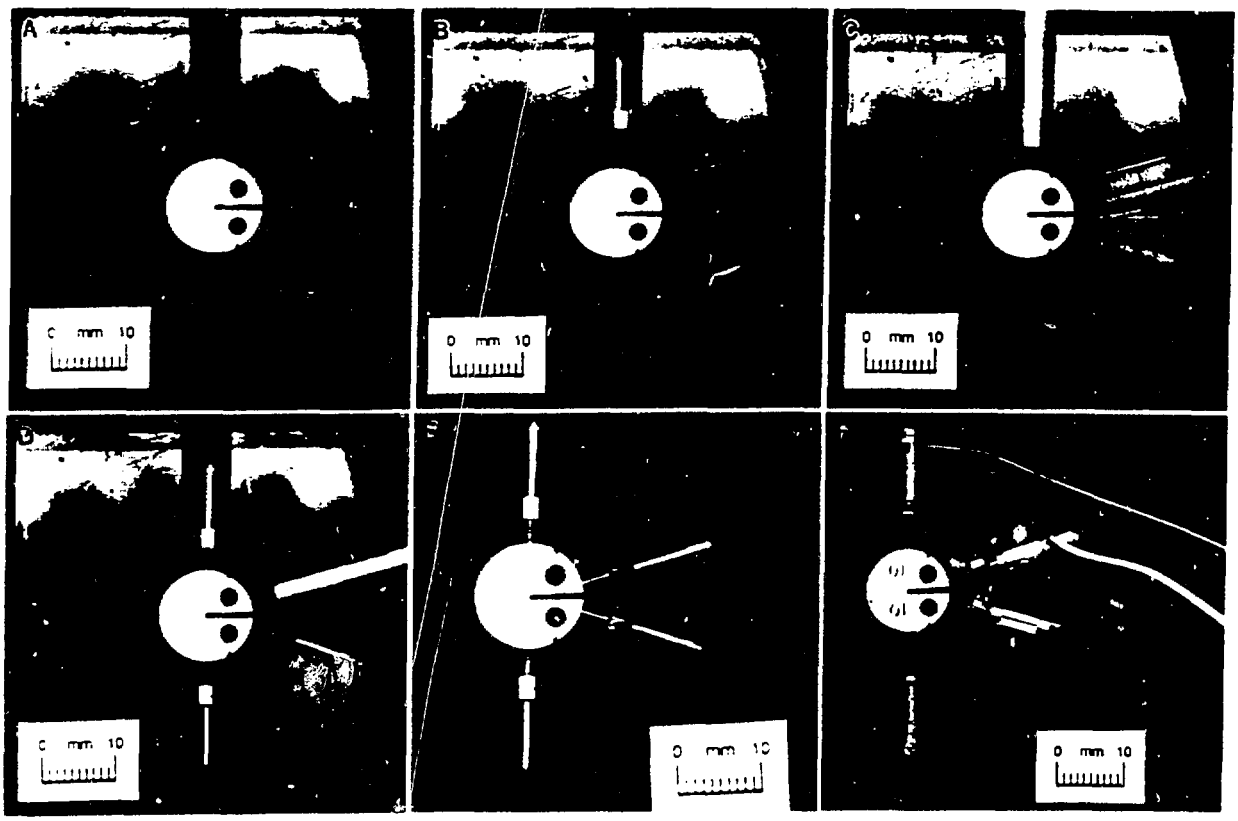

Fig. 4. The sequence of operations required for the attachment of the potential drop probes to the disk compact specimen.

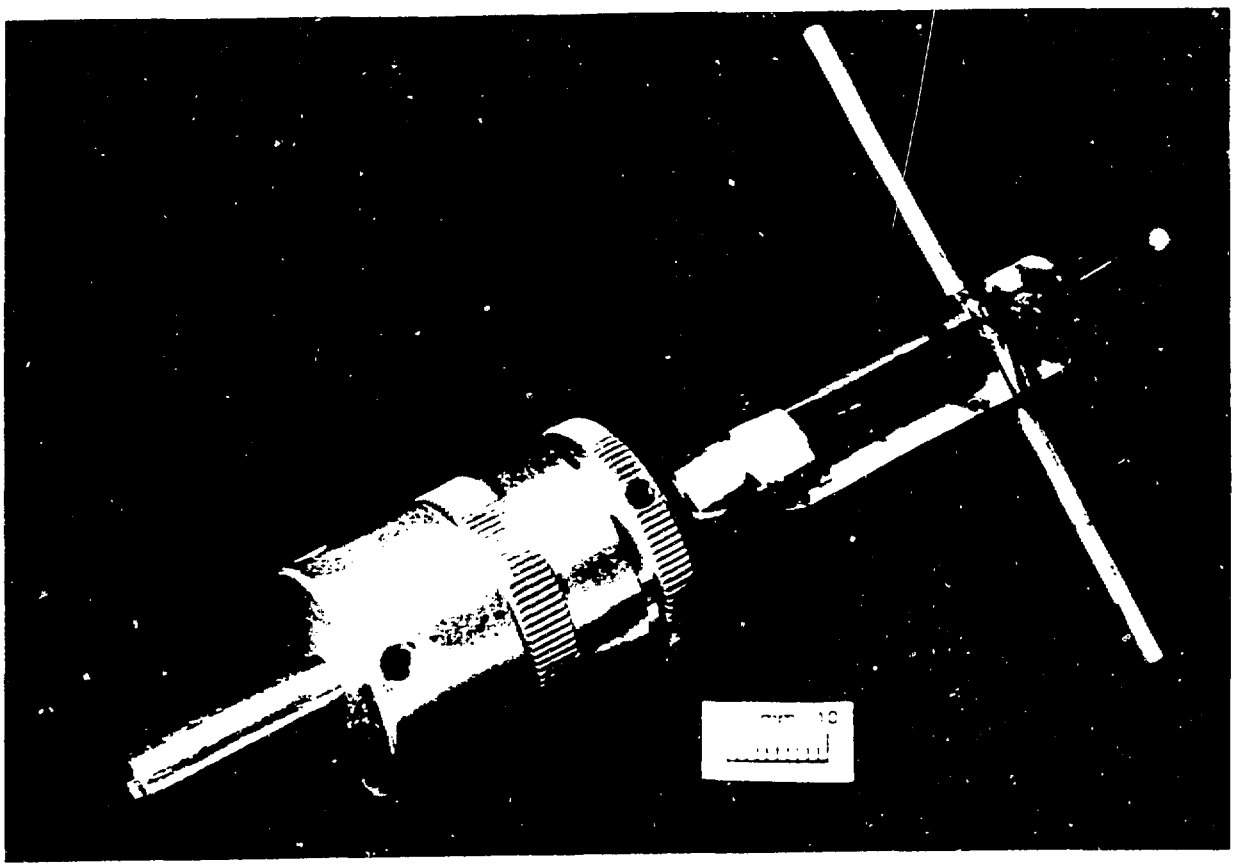

Fig. 5. The modified nutdriver used for attaching the probes to the disk compact specimen. Note the cross pieces at the end of the handle, and the slip coupling inserted on the shaft.

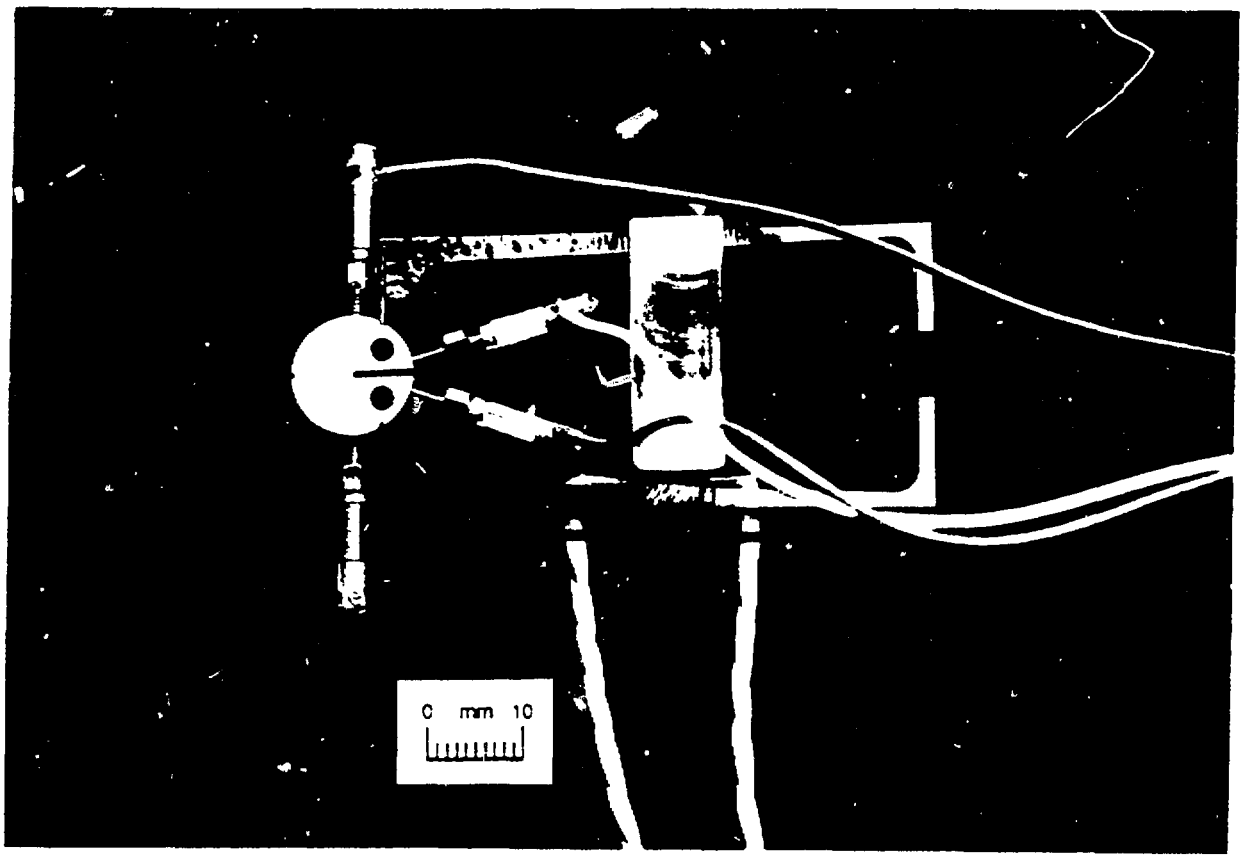

Fig. 6. A view of the complete assembly, showing the potential drop probes and lead wires, and the unloading compliance clip gage. The clip gage has a protective shield mounted over the middle flexural member, to protect the strain gages.

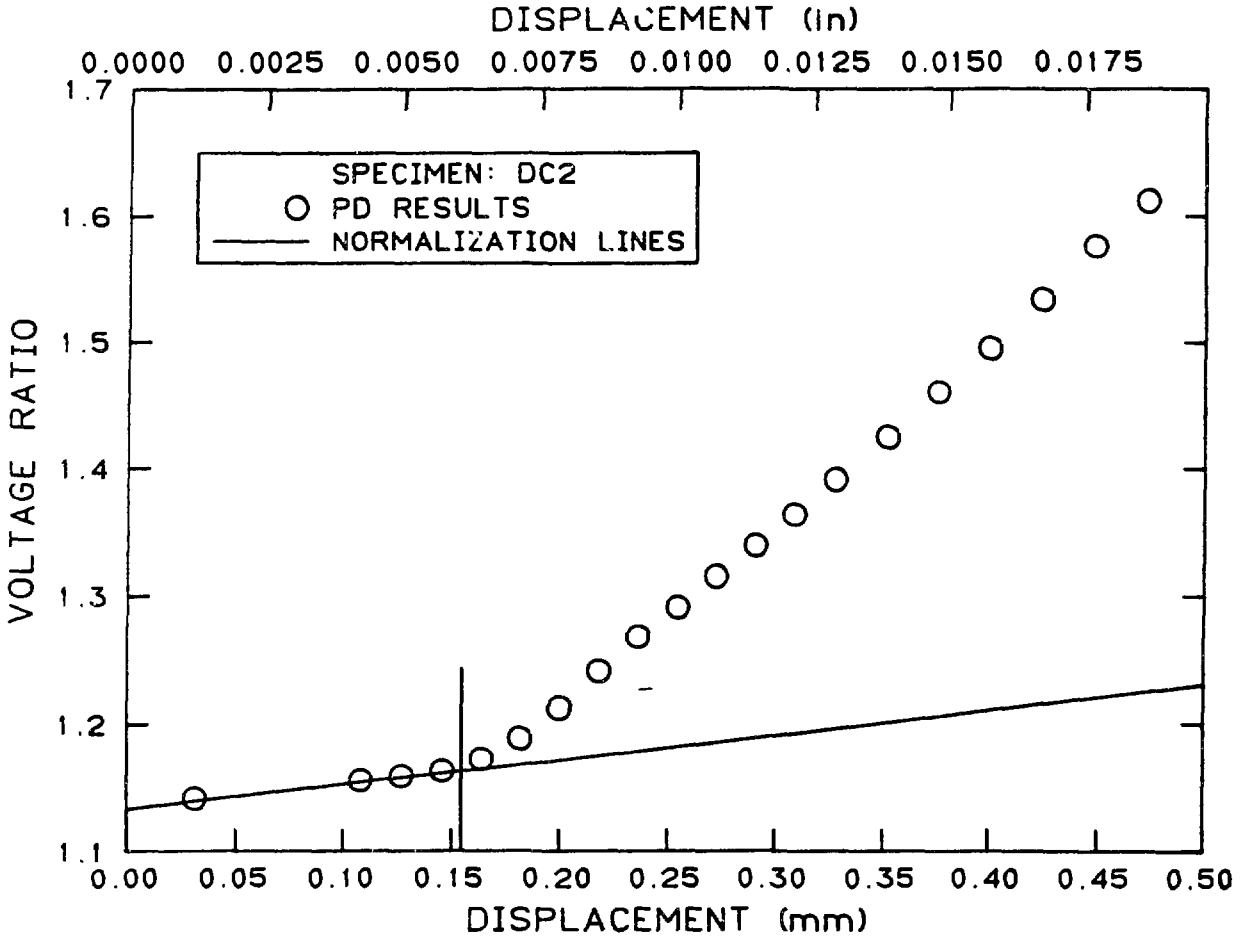

Fig. 7. A plot of the voltage ratio versus the load line displacement for one of the disk compact specimens. The straight line is used to assist the selection of the point of initial deviation from linearity. The vertical line shows the point selected as the beginning of crack extension.

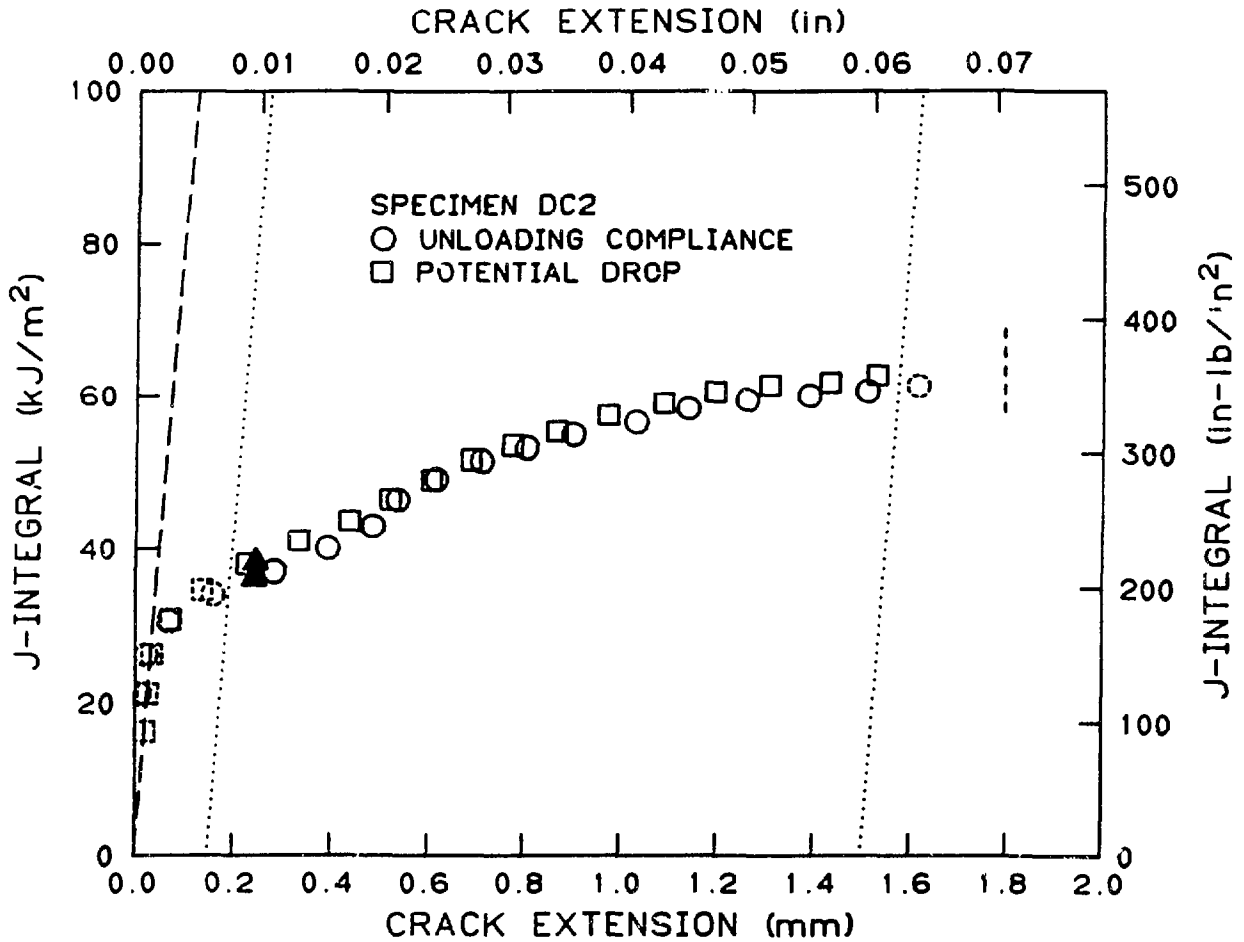

Fig. 8. An example of the J-R curve from a disk compact specimen, showing excellent agreement between the data from unloading compliance and that from potential drop. Both methods predict the measured final crack extension quite well.

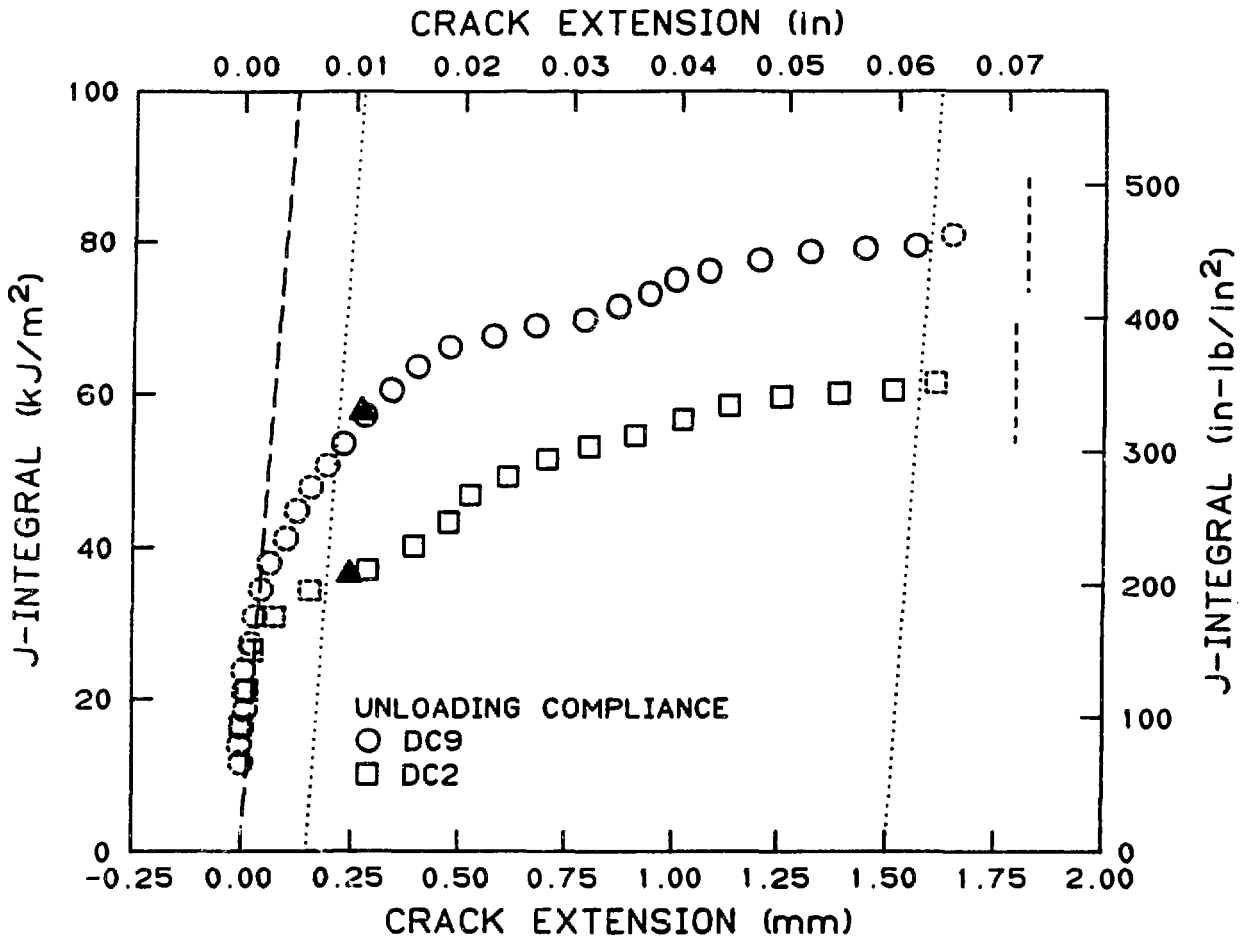

Fig. 9. J-R curves obtained by the unloading compliance technique from two apparently identical disk compact specimens, showing that some scatter was observed from replicate tests. Both tests showed good agreement between measured and predicted crack extensions.

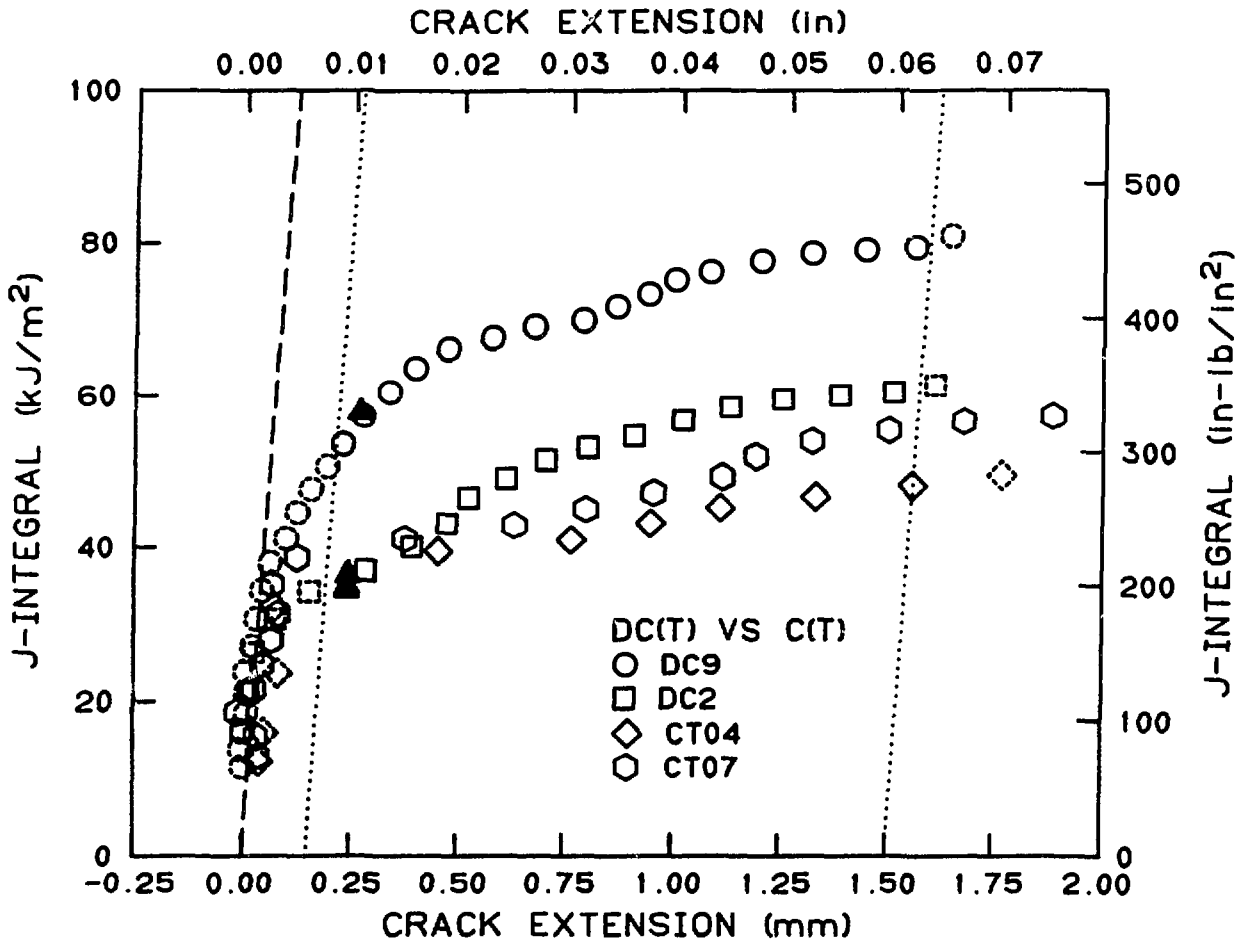

Fig. 10. A comparison between the J-R curves obtained by unloading compliance from 1/2 T compact specimens and the 0.18 T disk compact specimens. The compact specimens gave similar J_{Ic} values, but the J-R curves had lower slopes (lower tearing moduli).

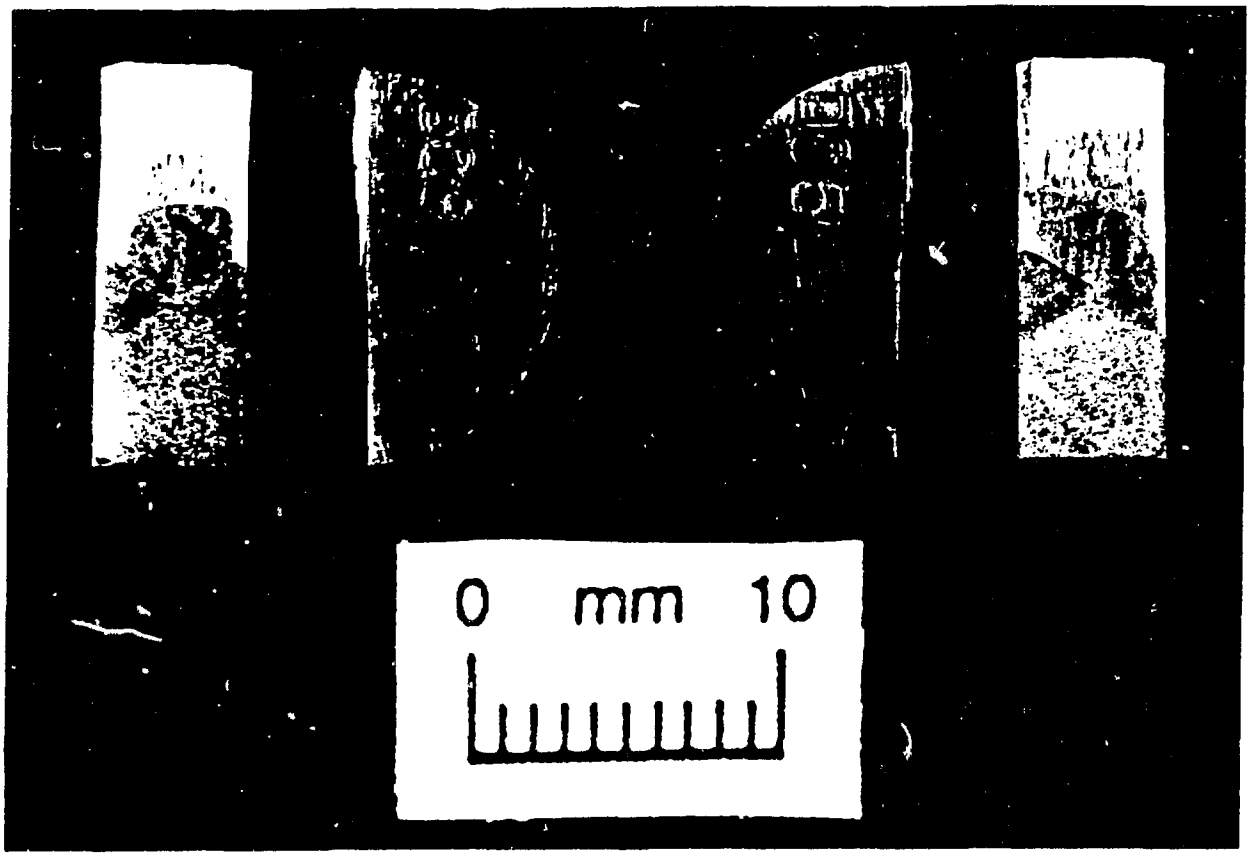

Fig. 11. Fracture surfaces from two of the disk compact specimens. Note the chevron notch to assist in precracking, and the sidegrooves added after precracking was finished. The fracture surface shows that crack growth occurred with slight tunneling, but there was little distortion of the specimens' shape.